International Immunopharmacology 9 (2009) 330–339

Contents lists available at ScienceDirect

International Immunopharmacology

journal homepage: www.elsevier.com/locate/intimp

# Immunodominant role of CCHA subunit of *Concholepas* hemocyanin is associated with unique biochemical properties

María Inés Becker [a,b,*], Alejandra Fuentes [a], Miguel Del Campo [a], Augusto Manubens [b], Esteban Nova [a], Harold Oliva [a], Fernando Faunes [a], María Antonieta Valenzuela [c], Marcelo Campos-Vallette [d], Alvaro Aliaga [d], Jorge Ferreira [e], Alfredo E. De Ioannes [b], Pablo De Ioannes [a], Bruno Moltedo [a]

[a] *Fundación Ciencia y Tecnología para el Desarrollo, Avenida Eduardo Castillo Velasco 2902, Santiago, Chile*
[b] *Biosonda Corporation, Avenida Eduardo Castillo Velasco 2902, Santiago, Chile*
[c] *Facultad de Ciencias Químicas y Farmacéuticas, Universidad de Chile. Olivos 1007, Santiago, Chile*
[d] *Facultad de Ciencias, Universidad de Chile. Las Palmeras 3425, Santiago, Chile*
[e] *Instituto de Ciencias Biomédicas ICBM, Facultad de Medicina, Universidad de Chile. Avenida. Independencia 1027, Santiago, Chile*

ARTICLE INFO

*Article history:*
Received 28 August 2008
Received in revised form 5 December 2008
Accepted 17 December 2008

*Keywords:*
Immunogen
Hemocyanin
*Concholepas concholepas*
CCHA and CCHB subunits characterization
Immunotherapy
Bladder cancer

ABSTRACT

Hemocyanin, the oxygen transporter metallo-glycoprotein from mollusks, shows strong relationship between its notable structural features and intrinsic immunomodulatory effects. Here we investigated the individual contribution of CCHA and CCHB subunits from *Concholepas* hemocyanin (CCH) to *in vivo* humoral immune response and their pre-clinical evaluation as immunotherapeutic agent in a mice bladder cancer model, in relation to their biochemical properties. To this end, subunits were purified and well characterized. Homogeneous subunits were obtained by anionic exchange chromatography, and its purity assessed by electrophoretic and immunochemical methods. While each CCH subunit contains eight functional units showing partial cross reaction, the vibrational spectral analysis showed several spectral differences, suggesting structural differences between them. In addition, we demonstrated differences in the carbohydrate content: CCHA had a 3.6% w/w sugar with both N- and O-linked moieties. In turn, CCHB had a 2.5% w/w sugar with N-linked, while O-linked moieties were nearly absent. Considering these differences, it was not possible to predict *a priori* whether the immunogenic and immunotherapeutic properties of subunits might be similar. Surprisingly, both subunits by itself induced a humoral response, and showed an antitumor effect in the bladder carcinoma cell line MBT-2. However, when immunologic parameters were analyzed, CCHA showed better efficiency than CCHB. No allergic reactions or any toxic effects were observed in mice treated with CCHA, sustaining its potential therapeutic use. Our study supports that CCHA subunit accounts for the most important features involved in the immunogenicity of CCH, such as better hydrophilicity and higher content of carbohydrates.



## 1. Introduction

There is a growing biomedical interest in hemocyanins, the respiratory metallo-glycoproteins of some mollusks, due to their remarkable immunogenicity and adjuvanticity *in vivo*. Their huge size, xenogenic character, carbohydrate content and sophisticated quaternary structure have been implicated in inducing strong immune responses in mammals [1].

Hemocyanins are formed by ten dissociable monomers or subunits that constitute a hollow cylindrical structure known as decamer. The molecular weight of the molluskan hemocyanin subunits is about 350 to 450 kDa. Each subunit contains eight globular domains (50 kDa) known as functional units (FUs) connected by a flexible linker strand of around 15 amino acid residues. Each FU has two copper atoms, each atom is coordinated to the protein by three highly conserved histidine residues [2]. Subunits can be arranged as hollow cylindrical of three-tiered decamers or in stable self-associated didecamers depending on species with an asymmetrical face-to-face interaction between decamers; resulting in colossal structures of 8 MDa or even bigger [3]. The three-dimensional reconstruction of these giant molecules reveals that decamers present $D_5$ like symmetry [4]. Dissociation studies on the mollusk hemocyanins demonstrated that subunits vary in composition and arrangement. Subunits can be homogeneous, consisting of a monomeric form, or heterogeneous, often containing two monomers encoded by different genes. In the last case, subunits can show exclusive association among single subunit types generating two

* Corresponding author. Fundación Ciencia y Tecnología para el Desarrollo, Chile. Tel.: +56 2 2096770; fax: +56 2 2745462.
*E-mail address:* mib@biosonda.cl (M.I. Becker).

1567-5769/$ – see front matter © 2008 Elsevier B.V. All rights reserved.
doi:10.1016/j.intimp.2008.12.011

homodecamers as the hemocyanin from *Megathura crenulata* known as KLH [5]. In contrast, subunits can also be intermingled, generating a heterodecamer, as is the case of hemocyanin from *Concholepas concholepas* known as CCH [6].

Since the pioneer work of Weigle in the 60 s on the immunochemical properties of KLH [7], this protein has been used as a model of thymus-dependent antigen. Afterwards KLH was used for the evaluation of immunological competence in humans. Nowadays KLH is widely used as a peptide-carrier either for the production of specific antibodies or for the induction of antigen specific $CD8^+$ and $CD4^+$ T cells [8]. Moreover, KLH has been successfully employed as carrier for carcinoma ganglioside and mucin-like epitopes in cancer immunotherapy [9–11] or as adjuvant when co-administered with dendritic cells (DCs) pulsed with T-lymphoma [12] or melanoma-lysates [13–16]. KLH has also been used as a nonspecific immunostimulant for the treatment of superficial bladder carcinoma [17,18]. However, KLH is poorly soluble, large and heterogeneous [19]. Therefore, there is a growing need for extremely immunogenic carrier proteins that are highly soluble, monomeric and homogeneous.

The present research focuses on the subunits of *Concholepas* hemocyanin. Previously, we reported that CCH is made up of two non-covalently linked subunits; CCHA (405 kDa) and CCHB (350 kDa) [6]. A comparative analysis between KLH subunits (KLH-1 and KLH-2) and CCH subunits, showed significant structural differences: CCH exhibits a heterodidecameric array of subunits that contain common and specific epitopes [20]. In contrast, KLH subunits form homodidecamers that do not display shared epitopes [21]. Moreover, purified KLH requires divalent cations in storage buffers to maintain stable quaternary structure while CCH does not, probably a consequence of its higher hydrophobicity [22]. In spite of these differences, the immunogenic properties of CCH are similar to KLH. The CCH has been successfully used as a carrier protein to produce antibodies against haptens and peptides [23–26], as carrier in vaccines [27,28] as well as experimental antigen [29]. Moreover, CCH is as effective as KLH in preventing tumor growth in a murine bladder cancer model [30].

Our long-term goal is to improve the understanding of the relationship between the structural features of hemocyanins and their intrinsic immunomodulatory effects. We propose that to identify these structural features, it is necessary to investigate in deep the properties of each subunit of these giant proteins. Accordingly, they should be well purified and characterized. To accomplish this, we isolated pure and soluble CCHA and CCHB monomers from *Concholepas* hemocyanin to identify their biochemical and structural properties and evaluate their potential immunogenicity and antitumor properties in a murine bladder cancer model *in vivo*.

## 2. Materials and methods

### 2.1. Biologicals

#### 2.1.1. Mice

BALB/c (H-$2^b$), C3H/He (H-$2^k$) and C57Bl/6 (H-$2^d$) mice strains were purchased from Jackson Laboratory (USA) and were breed at Biosonda Corp. All procedures were approved by the Institutional Animal Care ("Manual de Normas de Bioseguridad", edited by CONICYT in 2008).

#### 2.1.2. Cell line

The mouse tumor bladder cell line (MBT-2, donated by Dale Riggs, West Virginia University School of Medicine, USA), was cultured in Dulbecco's medium containing 10% FBS (HyClone, USA), 100 IU/ml penicillin, and 100 μg/ml streptomycin (Gibco, USA) at 37 °C in a 10% $CO_2$ atmosphere. The cells were harvested by short trypsinization, and after washing in culture media, cells were counted in a hemocytometer and viability was confirmed as >98% by trypan blue exclusion [30].

### 2.2. Purification of CCH subunits by anionic exchange chromatography

Hemocyanin from *C. concholepas* tested as LPS-free by the Quantitative chromogenic LAL assay (Bio Whittaker, USA) was provided by Biosonda S.A., Chile. All chemicals were analytical-grade and the solutions were prepared using lipopolysaccharide-free water from Baxter Healthcare, USA. The CCH subunits were purified according to De Ioannes et al. [6] with minor modifications. Briefly, all purification steps were carried out at 4 °C under a laminar flow chamber when possible. The glassware was depyrogenated by heat treatment. CCH was dialyzed in dissociation buffer (130 mM glycine–NaOH pH 9.6) at 4 °C. The dissociated CCH was applied on a Q-Sepharose (Pharmacia, Sweden) column (10×0.8 cm) equilibrated with the dissociation buffer and eluted by a linear gradient from 0.3 to 0.6 M NaCl (5 column volumes). Fractions were analyzed by SDS-PAGE, pooled and concentrated by centrifugation in the ultrafree system. Finally, isolated subunits were dialyzed against PBS and filtered thought 0.22 μm filter. Protein concentration was determined by the Bradford method [31]. The purity and homogeneity of each CCH subunits was determined by electron microscopy, diverse electrophoretic methods and western blot analysis using our anti-CCH subunits mAbs [20].

### 2.3. Electron microscopy

Samples were negatively stained with 1 to 2% aqueous uranyl acetate solution [6]. Grids were observed under a Phillips Tecnai 12 electron microscope at the Servicio de Microscopía Electrónica, Pontificia Universidad Católica de Chile.

### 2.4. Copper content and isoelectric point (pI)

Copper was determined by atomic absorption spectroscopy in GBC equipment (Model 902, Australia) with a hollow copper cathode lamp of 324.8 nm (Photon), at the Centro de Servicios Externos of the Pontificia Universidad Católica de Chile [6]. Isoelectrofocusing was carried out on 4% polyacrylamide gels in a Mini IEF Cell Model 111 (BioRad, USA) using 5 to 7 pH ampholites as described before [32].

### 2.5. Gel electrophoresis

SDS-PAGE was carried out using 3 to 12% separating gel and 3% stacking gel at 70 V for 12 h at room temperature using standard procedure [33]. Samples were heated for 5 min at 100 ° C with SDS and β-Mercaptoethanol. Proteins were visualized by Coomassie blue or silver staining [34].

The native electrophoresis of proteins was carried out in agarose gel using a horizontal gel chamber, on 1.5% agarose gels prepared in 70 mM Tris and 261 mM boric acid pH 7.4 (running buffer). Protein samples were diluted in the same buffer containing 50% glycerol and bromophenol blue. Electrophoresis was run at 20 V for 4 h at room temperature. Proteins were visualized by Coomassie blue staining.

### 2.6. Capillary electrophoresis

Capillary zone electrophoresis (CZE) was performed using an Ion Analyzer Capillary Electrophoresis system (Waters, Mildford, MA, USA) with Millenium software (Waters) for data handling [35]. Sample was applied by hydrodynamic injection (10 cm height, for 30 s) and detected at 185 nm. A fused-silica capillary (50 μm in diameter and 68 cm long) was used and the Electrophoretic analysis was performed at 18 kV at 25 °C using 150 mM phosphoric acid (pH 1.5) as the running solution. The capillary column was washed sequentially by 3-min injections of 0.5 M NaOH, distilled water, and running electrolyte prior to each run.

### 2.7. Immunoelectrophoresis (IE-2D)

The IE-2D experiments were performed according to Walker [36]. For the first dimension, samples (20 μg) were loaded on 1% agarose slab gel equilibrated in 0.03 M barbitone buffer, pH 8.4 and run at 20 mA for 1 h at 4 °C. For the second dimension, a slab gel consisted of 10 ml of agarose gel containing 300 μl of anti-CCH rabbit sera developed in our laboratory. The gel was run overnight at 5 mA for 12 h at 4 °C, it was sequentially washed with PBS, Milli-Q water and stained with 0.1% Amido black, 50% methanol and 10% acetic acid.

For FUs analysis, pure subunits were digested with pancreatic elastase according as described by others [5,37]. Pancreatic elastase (2% w/w) was dissolved in 1 ml of 0.1 M ammonium-carbonate pH 8.0, and added to a solution containing 20 mg of subunits in glycine–NaOH 0.13 M pH 9.6, and incubated at 37 °C for 5 h. Protein fragments were analyzed by SDS-PAGE. As control, a similar sample was incubated without the enzyme.

### 2.8. Western blot analysis

The procedure described by Towbin et al. [38] was used. Samples (10 μg) were separated on a 3 to 10% SDS-PAGE gel, and then transferred to a nitrocellulose membrane. The membrane was blocked overnight with 1% Casein in PBS, and then developed with specific anti-CCH subunits mAbs as described previously [20]. Briefly, the membranes were incubated for 3 h with undiluted hybridoma supernatants. After washings with PBS–Tween 0.02%, the membranes were incubated during 1 h at room temperature with goat anti-mouse IgG serum, conjugated with ALP. The membranes were developed using NBT and BCIP system. The reaction was stopped by washed with water.

### 2.9. Surface enhanced Raman spectroscopy (SERS)

Colloidal silver nanoparticles were prepared using hydroxylamine hydrochloride as reducing agent [22]. Metal films of Ag nanoparticles for micro-SERS measurements were prepared by immobilization of colloidal nanoparticles. Previously, an aliquot of the protein in PBS was added to 500 μl of silver colloid to desired concentration, and then it was activated by addition of 0.5 M aqueous potassium nitrate to a final concentration in the range $10^{-2}$–$10^{-3}$ M. Then, 20 μl of the final suspension was deposited onto a glass cover slide and dried at room temperature. The SERS spectra (using a 50× objective) were recorded with a Renishaw Raman Microscope System RM1000 equipped with the 514 nm laser line, microscope and an electrically refrigerated charge-coupled device camera, and a notch filter to eliminate the elastic scattering. The output laser power was in the range 0.1–2.0 mW. Spectral resolution was 2 $cm^{-1}$. The spectral scanning conditions were chosen to avoid denaturation of protein.

### 2.10. Sugar moieties analysis

To determine the presence of carbohydrates on each subunit of CCH, the periodate oxidation method was used [39]. Briefly, each protein (0.5 mg/ml) was dissolved in 0.1 M acetate buffer pH 5.5 containing 15 mM sodium periodate (fresh) and incubated 1 h in the dark at room temperature, then 25 ml of ethylene glycol were added and left overnight at 4 °C. The reactive aldehydes were detected by biotin–streptavidin–ALP method [40]. Percentages of sugar moieties were determined enzymatically using a commercial kit (SIGMA, USA), according to the manufacturer's instructions. Fetuin was included as positive control [41]. The extent of deglycosylation was determined by the shift in the protein band mobility on SDS-PAGE gels silver stained.

The nature of sugar moieties present on the proteins was determined with the biotinylated lectins concanavalin A (ConA) and peanut agglutinin (PNA) in a dot-blot assay [42]. Sample (20 μg) was placed on the nitrocellulose membrane, and blocked with 3% Casein. The membranes were incubated with biotinylated lectins (1 μg/ml) and then, with 0.1 units streptavidin–ALP (Vector Lab.). Finally, membranes were developed with NBT-BCIP (Pierce, USA). For controls, deglycosylated CCH was used.

### 2.11. Immunization, experimental schedule and ELISA

Two-month-old BALB/c, C3H/He or C57BL/6 mice were used. We immunized three mice per group as follows: on day 1 they received intraperitoneally 400 μg of CCHA or CCHB subunits in 100 μl sterile endotoxin-free PBS. A similar dose of whole CCH or only PBS was used as positive and negative control, respectively. On day 15, the same immunization was carried out. Ten days after the second antigen injection, mice were bled and sera obtained. Mice were bled prior to the immunizations to obtain pre-immune control serum.

The presence of specific IgG antibodies in mice serum was detected by ELISA [43]. 96-well plates (Pierse-Endogen, USA) were coated by adding of 100 μl/well of CCHA, CCHB or whole CCH at 10 μg/ml in PBS and incubated overnight at 4 °C. The plates were blocked 2 h at room temperature with 1% BSA in PBS and then washed with 0.02% PBS-Tween. Then, serial half dilutions of the immune sera of mice in 1% BSA in PBS were incubated for 2 h at 37 °C. The plates were washed three times with 250 μl of 0.02% PBS-Tween and subsequently, 100 μl/well of goat anti-mouse IgG serum conjugated with ALP (1/2000 dilution) in blocking buffer was added to the wells. After incubating for 30 min at 37 °C, the plates were washed and developed by adding 100 μl/well of 1 mg/ml para-NPP in ALP-buffer ($Na_2CO_3$/$NaHCO_3$ 0.2 M, pH 9.6). The reaction was stopped with 3 N NaOH and was read spectrophotometrically at 405 nm. Individual antibody titers were determined. The titer was defined as the reciprocal of the serum dilution showing the half of the maximum absorbance at 405 nm.

The results of experiments are expressed as mean ± standard error (SE). Comparison between groups was done by the Two-way ANOVA test and Bonferroni post-test. Probability values $p<0.05$ were considered significant.

### 2.12. Immunotherapy and experimental schedule

Two-month-old C3H/He mice were challenged with MBT-2 cells, according to Moltedo et al. [30]. Briefly, two weeks prior to the tumor implantation, groups of five to nine mice were randomized and primed intradermally with 200 μg of CCHA or CCHB subunits in 100 μl sterile endotoxin-free PBS; similar groups of mice were treated with 200 μg of whole CCH or 100 μl PBS, as positive and negative control, respectively. After day 15, mice were challenged with a subcutaneous injection of 200,000 MBT-2 cells in 100 μl Dulbecco's 0.1% FCS, into the right flank. Immunotherapy (100 μg each subunit in 100 μl PBS per dose) was administered on alternated days for 9 days after the challenge with tumor cells, with a cumulative dose of 500 μg. A similar schedule was used in controls. The tumor incidence was evaluated by visual inspection and palpation. Tumor dimensions (length and width) were measured every 3 to 5 days, for up to day 25, previous to the exponential growth of the tumor. Tumor volume was calculated using the ellipsoid formula ($Volume = 0.52 \times L \times W^2$). The survival of mice was recorded over a period of 70 days. Mice were screened for internal tumor by gross visual inspection of organs upon death.

The results of experiments are expressed as mean ± SE. Comparison between groups was done by the Two-way ANOVA test and Bonferroni post-test. Survival rate was estimated by the Kaplan–Meier method and log-rank test. Analyses were performed using GraphPad Prism software (GraphPad software, Inc., San Diego, CA).

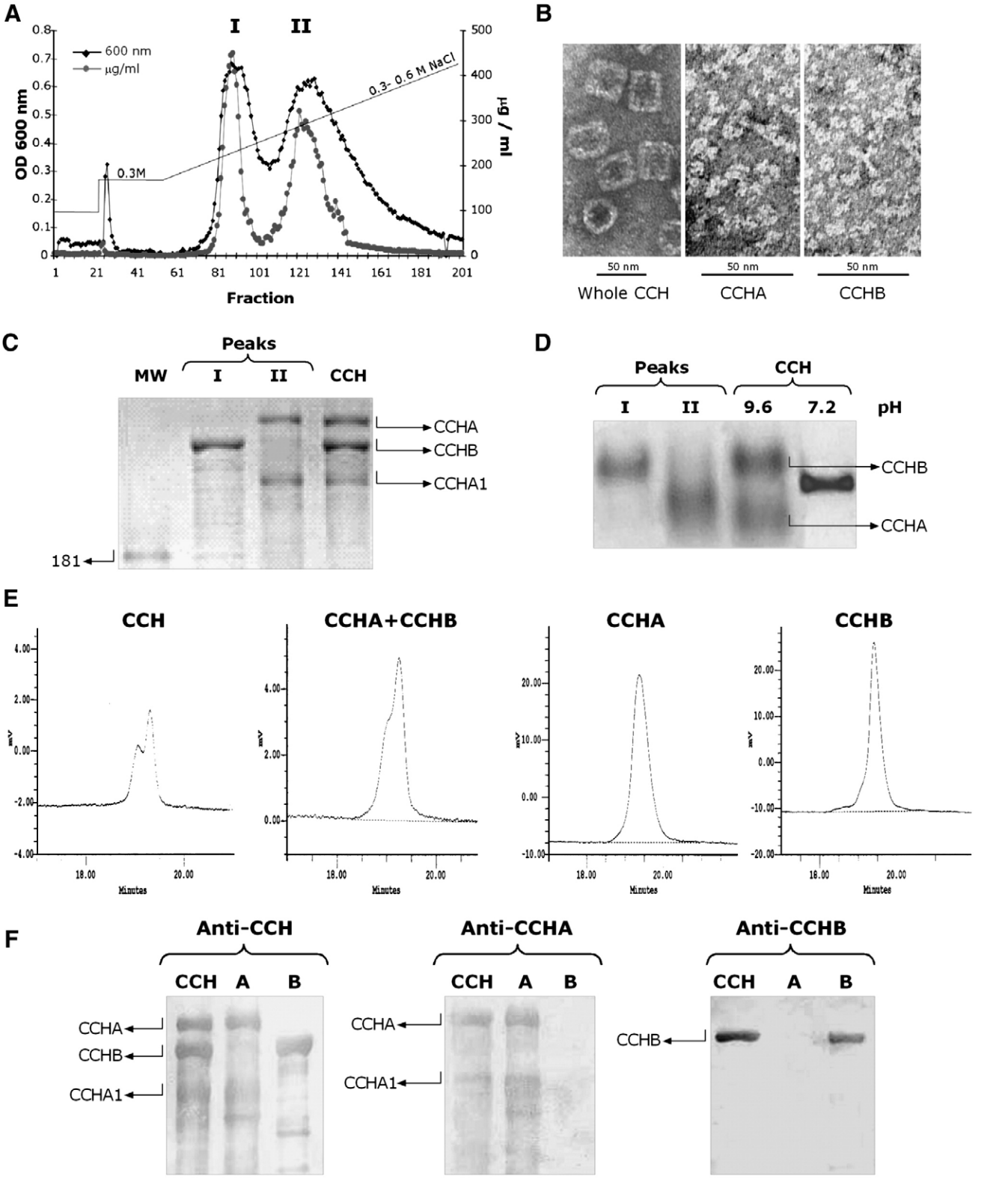


**Fig. 1.** Purification of isolated subunits from *C. concholepas* hemocyanin. (A) Chromatographic profile of CCH previously dissociated, showed two different peaks named I and II. (◆) Protein profile at 600 nm. (●) Protein concentration. (B) Electron microscopy of purified subunits of CCH negatively stained. CCH molecules as control, showing their characteristic didecameric form: top (circles) and lateral (rectangles) views of the protein. In contrast, the purified CCHA and CCHB subunits have lost the quaternary structure. (C) SDS-PAGE analysis under reducing conditions of the fractions obtained in the Q-Sepharose column. Lanes were loaded from the left to right with: molecular weight markers standards, peak I fractions corresponding to CCHB (350 kDa), peak II fractions corresponding to characteristic CCHA bands (CCHA 405 kDa and CCHA1 300 kDa), and CCH used to dissociate subunits as control. (D) Native gel electrophoresis in agarose gel. Lanes were loaded from the left to right with: Fractions of peak I showed a polypeptide corresponding to CCHB subunit. Peak II fractions showed one polypeptide corresponding to the CCHA subunit. CCH dissociated showed both d subunits. CCH in PBS (pH 7.2) as control, showing one compacted band. (E) Capillary electrophoresis showing the electropherograms at 185 nm obtained by whole CCH molecule showing two overlapped peaks. Also two overlapped peaks were observed when isolated CCH subunits were mixed previously to put in the capillary. One symmetric peak was observed in each isolated monomer. (F) Western blot analysis using polyclonal antibodies to CCH as positive control, and specific anti-CCH subunits mAbs (anti-CCHA 4C10, and anti CCHB 2H10) [20]. CCHA subunit does not show the characteristic band of CCHB subunit and vice-versa, confirming the purity of each monomer.

## 3. Results

### 3.1. Fractionation of whole CCH yields soluble and pure CCHA and CCHB monomers

To obtain highly purified CCH subunits devoid of cross contamination, CCH was equilibrated at pH 9.6, applied to Q-Sepharose column, and eluted with a linear 0.3 to 0.6 M NaCl gradient for sample elution. Two symmetric peaks (I and II) were observed suggesting elution of homogeneous monomers (Fig. 1A). The electron microscopic analysis by negative staining confirmed the isolation of dissociated subunits (Fig. 1B). SDS-PAGE analysis showed that peak I contained CCHB monomer while peak II contained CCHA monomer (Fig. 1C). Agarose gels showed homogeneous subunits and also, differences in the migration pattern between subunits (1d). The homogeneity of each subunit was assessed by capillary electrophoresis and electropherograms at pH 1.5 using an uncoated bare, fused-silica capillary are shown in Fig. 1E. One peak at 185 nm was observed for each species, and two for the controls (either the whole CCH molecule or CCHA previously mixed with CCHB in equal parts at the moment to load the capillary). Finally, western blot confirmed the recovery of pure subunits (Fig. 1F). The p*I* of CCHA and CCHB were 4.77 ± 0.024, and 4.93 ± 0.027, respectively (data not shown).

### 3.2. Immunochemical analysis and copper content confirmed that CCH subunits contains eight FUs

The FUs present in each subunit were determined by immunoelectrophoresis with anti-CCH rabbit antibodies. The results of IE-2D with whole CCH, showed that both CCH subunits share immunological identity (Fig. 2A). To determine the size of FUs, each subunit was digested with elastase, and subsequently the size of proteolytic fragment was assessed by SDS-PAGE. The results showed bands in the range of 50 kDa for CCHA and CCHB which exhibited the expected migration for intact FUs (Fig. 2B, arrows). CCHB, showed bands of less than 40 kDa,

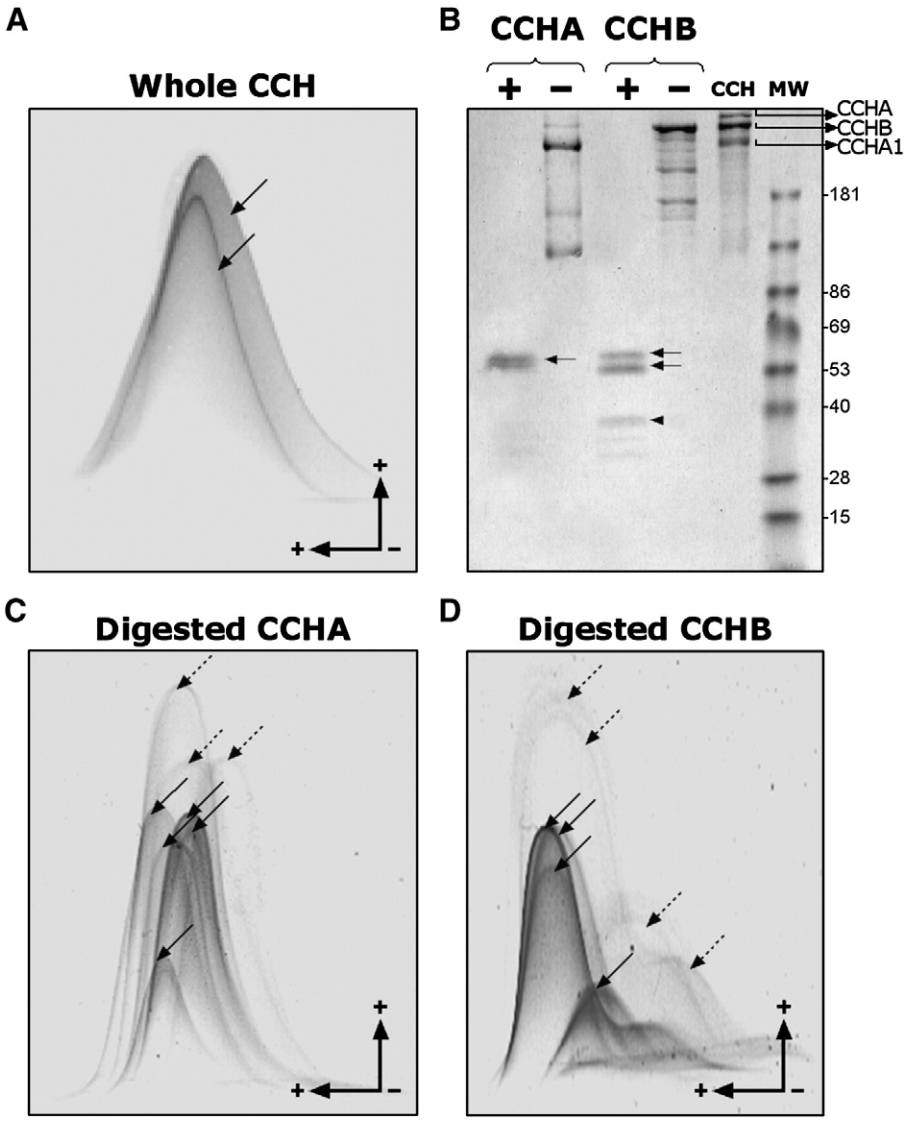


**Fig. 2.** Subunit organization of *C. concholepas* hemocyanin. (A) IE-2D analysis of CCH. In the first dimension whole CCH was run in an agarose gel under native conditions, and then the sample was subjected to a second dimension electrophoresis in an agarose gel containing anti-CCH antibodies. Two partially cross-reacting precipitin arcs, visualized with Amido black staining is shown (arrows). (B) SDS-PAGE analysis of elastase digested products of purified CCH subunits. (+) Subunits treated with elastase. The main polypeptides obtained after the digestion of subunits are shown. Bands in the range of 50 kDa (arrows) for CCHA and CCHB which exhibited the expected migration for intact FUs. Band of less than 40 kDa (arrowhead) for CCHB. (−) CCHA or CCHB subunit without elastase treatment. Non-digested CCH was included as control; at the end of gel molecular weight markers. (C) IE-2D of CCHA previously subjected to elastase digestion and run as in A. Eight partial cross-reacting precipitin arcs stained with Amido black are shown (arrows). Weak immunoreactions against FUs appear as punctuated arrows and strong immunoreactions appear as continuous arrows. (D) Analogous to C but for CCHB, where IE-2D of previously digested CCHB subunit show 8 precipitin arcs.

suggesting the existence of some smaller FUs (Fig. 2B, arrowhead), in agreement with previous observation on the smaller molecular size of CCHB (350 kDa) as compared with CCHA (405 kDa). To confirm the above observation, we analyzed the elastase digestion products of each subunit by IE-2D, and eight precipitin lines for both subunits were observed, and as expected some of them exhibited partial cross-reaction (Fig. 2C and D). Curiously, various weak immunoreactions against FUs in both subunits (punctuated arrows) were observed when compared with strong immunoreactions against FUs (continuous arrows). We assume that these weak and strong precipitin arcs represent low and high affinity anti-subunits FUs antibodies in the anti-CCH sera.

In addition, the copper content of each subunit was about 0.27% by weight, corresponding to a molar ratio of 16.2 copper mol/mol of CCHA subunit, and 15.4 copper mol/mol of CCHB subunit. This indicates that each monomer contains eight functional units, confirming the IE-2D analysis.

### 3.3. SERS spectra suggest structural differences among the CCHA and CCHB monomers

The SERS spectra of the CCH subunits and the whole CCH molecule are presented in Fig. 3, Table 1 shows the most probable assignment of bands. Each subunit shows only one spectrum confirming their homogeneity. The presence of a specific band for each subunit, involving conformationally sensitive Raman amide III and I modes, indicates structural differences between the CCH subunits. More specifically, these modifications involve amide III modes situated at 1268 $cm^{-1}$ in CCHA, and near 1270 $cm^{-1}$, displayed as a shoulder, in CCHB. This mode is observed at 1277 $cm^{-1}$ in the spectrum of CCH molecule. The amide I mode at 1625 $cm^{-1}$ in CCHA is observed in CCHB at 1600 $cm^{-1}$ as a large band, this mode is not clearly present in the spectrum of CCH. Several bands are observed in the spectra of both subunits, and CCH species, as a shoulder near 1650, 1600, 1581, 1330, 1212, 1150, 822, 769 and 663 $cm^{-1}$ (frequencies of CCH) with differences in intensity and frequency. These results can be interpreted in terms that the corresponding aminoacidic chemical functions that are structurally situated far from the CCHA-CCHB subunit interaction site. The corresponding aminoacidic conformations of such moieties are slightly modified by the parental CCH whole molecule. Another group of bands belonging to precursors CCHA and CCHB subunits at 1506 $cm^{-1}$ in CCHA and 1516 $cm^{-1}$ in CCHB, and 1289, 925 and 437 $cm^{-1}$ in CCHA, were not observed in the CCH spectrum; suggesting that they belong to amino acid residues involved in the CCH assembly. These moieties could be conformationally reoriented or chemically modified by the CCH formation. Bands at 1506, 1289, 925 and 437 $cm^{-1}$ are characteristics of the structure and conformation of CCHA subunit and should be useful for its identification. One of the most intense bands (1027 $cm^{-1}$) observed is present on the spectrum of the CCH molecule while the relative intensity of other CCH bands is progressively higher in the series (1330, 1405 and 1434 $cm^{-1}$). Both spectral behaviors are a consequence of a particular orientation of tryptophan which those bands were ascribed. Thus, the band at 1027 cm $^{-1}$ characterizes the CCH protein association.

**Table 1**
SERS frequencies ($cm^{-1}$) of CCHA and CCHB subunits, and bands assignment

| CCHA | CCHB | Most probable assignment |
|---|---|---|
| 1625 | | Amide I |
| 1599 | 1600 | Tyr, Phe |
| | 1572 | Trp |
| 1506 | 1516 | Hys |
| 1452 | 1473 | Amide II |
| 1430 | 1401 | Trp |
| 1352 | | Asp, Glu |
| 1336 | 1339 | Trp |
| 1289 | 1268 | Amide III |
| 1238 | 1233 | Amide III |
| 1210 | 1208 | Trp, Phe |
| 1155 | 1153 | Tyr, Phe |
| 1118 | 1101 | νC-N |
| 1051 | 1019 | Phe, Trp |
| 925 | 952 | νC-C |
| 829 | 841 | Tyr |
| 778 | 726 | Skeletal deformation |
| 698 | 684 | Cys |
| | 544 | Cys |
| 437 | | Skeletal deformation |

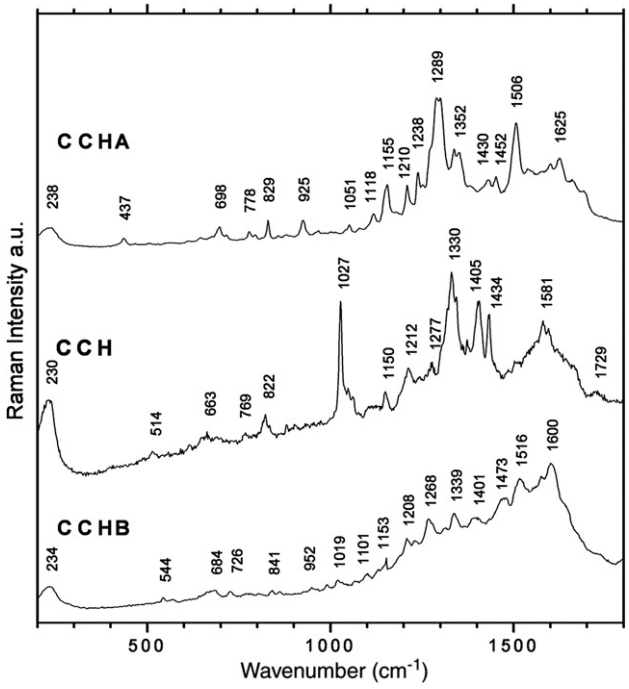


**Fig. 3.** Surface enhanced Raman scattering of subunits from *C. concholepas* hemocyanin. The spectra, employing a 514 nm laser with a Raman microscope (50× objectives), show the characteristic bands obtained with CCHA, CCHB and whole CCH on colloid silver. The main vibrational modes of the molecules are marked. The working range was 4000 to 50 $cm^{-1}$, and the assignments of the peaks are contained in the Table 1. The spectrum was baseline corrected, and the resolution was 2 $cm^{-1}$. The *y* axis is expressed in arbitrary units.

### 3.4. Sugar moieties content analysis indicated differences between CCHA and CCHB subunits

First, we investigated the presence of carbohydrate on CCH subunits using periodate oxidation, and developing the aldehyde groups

**Table 2**
Sugar content in % w/w of the subunits of C. *concholepas* hemocyanin

| Protein | Treatment | Sugar content[a] | |
|---|---|---|---|
| | | % w/w | % Sugar |
| CCHA | N-Glycosidase | 98.8 | 1.2 |
| | Glycosidase cocktail[b] | 96.4 | 3.6 |
| | O-linked | ND[c] | 2.4[d] |
| CCHB | N-Glycosidase | 97.7 | 2.3 |
| | Glycosidase cocktail | 97.5 | 2.5 |
| | O-linked | ND | 0.2 |
| Fetuin, control[e] | N-Glycosidase | 81.2 | 18.8 |
| | Glycosidase cocktail | 78.5 | 21.4 |
| | O-linked | ND | 2.6 |

[a] The values represent the average of 3 independent experiments, with a variation of less than 10%.
[b] Glycosidase cocktail signifies the presence of N-linked and/or O-linked glycans.
[c] ND, not determined.
[d] The % O-linked moieties not were determined, is an estimative value (difference among the % of sugars obtained with glycosidase cocktail minus N-Glycosidase treatments).
[e] Spiro and Bhoyroo [41].

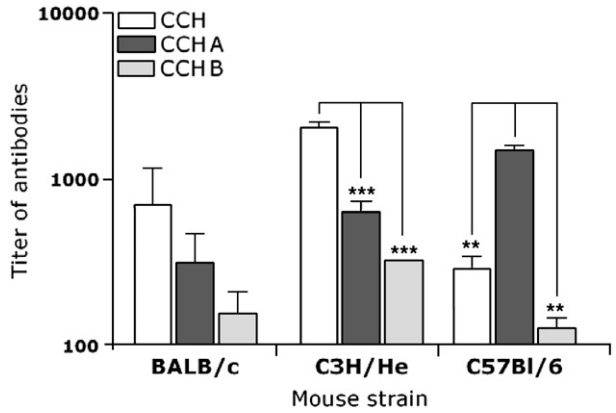


**Fig. 4.** Secondary humoral immune response against CCHA and CCB subunits in different mice strains by ELISA. Groups of 3 BALB/c, C3H/He or C57Bl/6 mice were immunized with CCHA or CCHB subunits in PBS, and whole CCH as positive control. The negative control with PBS (vehicle) was omitted in the figure. The samples of sera were taken 10 days after secondary injection and the presence of specific IgG antibodies was determined using an anti-mouse IgG-ALP sera. The reaction was developed with pNPP and read at 405 nm. The first dilution corresponds to 1:50. Data of three independent experiments are provided and shown the antibody titer as the mean ± S.E. The titer was defined as the reciprocal of the serum dilution showing the half of the maximum absorbance at 405 nm. Two-way ANOVA, BALB/c mice $p=0.0504$ for CCH *vs* CCHA and CCHB. C3H/He mice $p<0.01$ CCH *vs* CCHA and CCHB. C57Bl/6 mice $p<0.01$ CCHA *vs* CCH and CCHB.

by biotin–streptavidin–ALP. The results demonstrated that both CCH subunits are glycosylated (data not shown). Then, the sugar moiety content of each CCH subunit was analyzed by a shift in the electrophoretic mobility of the subunits after removal of all sugars. Accordingly, N-glycosidase and a glycosidase cocktail were used to remove N-linked or O-linked glycans, respectively and the results are shown in the Table 2. The sugar content of CCHA monomer was 3.6% w/w including both N-linked and O-linked moieties (1.2% w/w and 2.4% w/w, respectively. The CCHB monomer contained 2.5% w/w sugar corresponding to N-linked moieties, while O-linked oligosaccharides were almost absent (2.3% w/w and 0.2% w/w, respectively). To validate this technique Fetuin was used as control and a value of sugar moieties of 21.4% w/w was obtained as reported earlier.

To approach the nature of the carbohydrates moieties present on CCH subunits we used two common lectin enzyme conjugates in a dot-blot assay. Both, CCHA and CCHB showed clear reactivity with ConA which is specific for α-mannose, the major carbohydrate component of N-linked glycosides. In contrast, PNA which binds to disaccharide galactose (β1-3)-N-acetylgalactosamine, the core complex in O-linked glycoside, was almost negative (data not shown). These results are partially in agreement with the data on Table 2. Based on the knowledge on glycoprotein's structure, we support the notion that the arrangement of the O-linked glycans on CCH subunits may exert an effect on their availability by PNA binding sites [44].

### 3.5. CCHA subunit is more immunogenic than CCHB subunit

To compare the intrinsic immunogenicity of each isolated CCH subunit, the secondary antibody immune response was determined in the BALB/c, C3H/He and C57Bl/6 mice strains immunized either with soluble CCHA or CCHB; whole CCH or PBS were used as the positive and negative control, respectively. The primary response against these antigens was usually low (data not shown); hence, the presence of specific IgG antibodies in the mice sera was analyzed by ELISA. No detectable antibodies against the above antigens were found in mice sera prior to immunization. The Fig. 4 shows that both subunits by themselves induced the production of specific antibodies in all mice strains tested. Surprisingly the intensity of the humoral immune response against CCHA subunit was usually 3 times (BALB/c and C3H/He) to 10 times (C57Bl/6) higher than the CCHB, and even higher than the whole CCH molecule. The C57Bl mice showed titers 6 times higher with CCHA subunit than whole CCH. Similar results were obtained in two series of independent experiments. These differences were not due to dissimilar subunit binding on the ELISA plate (data not shown). In addition, both male and female mice responded in a similar way to the above antigens.

### 3.6. CCHA subunit might play an immunodominant role in antitumor effect of Concholepas hemocyanin

To determine the antitumor effect of both CCH subunits, the MBT-2 heterotopic murine bladder carcinoma model was used. Several different protocols have been used to study the antitumor activity of potential pharmacological substances using murine bladder cancer models. For instance, the number of tumor cells used in subcutaneous or intravesical challenge experiments ranged from 1000 to 2,500,000 cells *per* animal; treatment with hemocyanins was given with different schedules, with or without preimmunization, with doses ranging from 10 mg to 1.000 mg, with or without priming [30,45]. Hence, the choice of the immunization protocol was based in our previous work, where number of MBT-2 cells, dose and time interval of immunotherapy with whole CCH and KLH were established [30]. Accordingly, the C3He/He mice were primed subcutaneously with

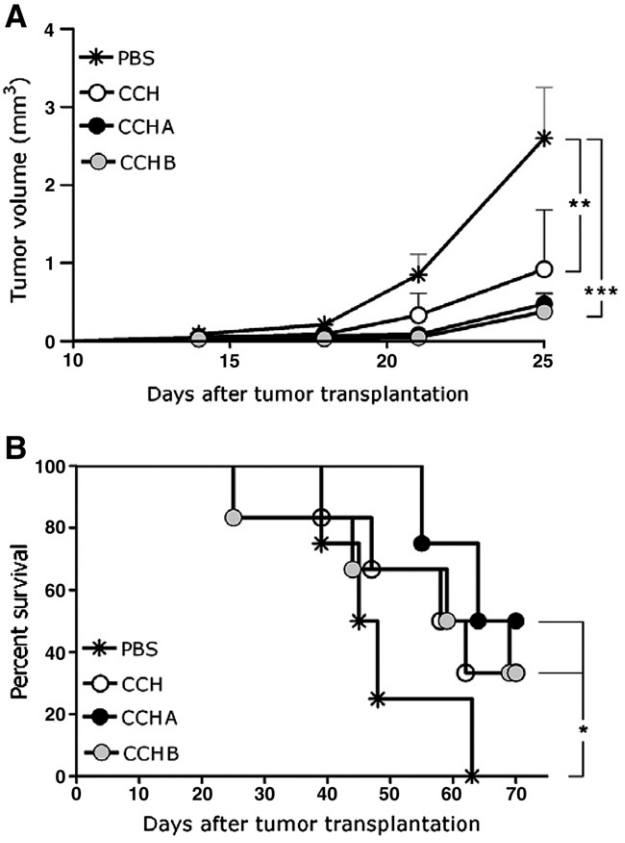


**Fig. 5.** Antitumor activity of the CCH isolates subunits. (A) Groups of mice (5 to 9 mice/group) were subcutaneously immunized with CCHA or CCHB subunits in PBS, and whole CCH or PBS as positive and negative control, respectively. Mice challenged subcutaneously with 200,000 MBT-2 cells. Tumor size was measured every 3 to 5 days and tumor volume was calculated using the ellipsoid formula. The immunotherapy schedule was 100 mg hemocyanin per dose on alternate days during 9 days. At day 25 a significant decreased of tumor growth is observed in mice treated with hemocyanin subunits when compared with PBS group. Representative data of two separate experiments are shown. $p<0.001$ PBS *vs* CCHA and CCHB, $p<0.01$ PBS *vs* CCH. (B) A Kaplan–Meier survival curve showed that animal death was retarded with hemocyanin subunits treatments, $p<0.05$ PBS *vs* CCHA, CCHB, and whole CCH.

CCHA, CCHB or whole CCH and PBS, as positive and negative controls, respectively; after day 15, mice were challenged with a subcutaneous injection of 200,000 MBT-2 into the right flank and the antitumor treatment was started: a subcutaneous dose of each subunit or controls on alternate days for 9 days.

The results correspond to representative experiment, of two independent experiments, are shown in Fig. 5. Before the exponential growth of the tumor, up to day 25, immunization with both CCHA and CCHB subunits, significantly slowed the tumor growth rate, as whole CCH used as positive control, compared with to the PBS group (Fig. 5A). Concomitantly, tumor incidence was lower in animal treated with hemocyanins: CCHA (44% incidence), CCHB (60% incidence) and whole CCH (62.5% incidence). At this time, 100% PBS control mice exhibited palpable tumors. Survival probability was significantly higher in mice treated with hemocyanins (either with monomers or the whole molecule) compared to PBS controls (Fig. 5B). All mice in the PBS control group were dead by day 70. However, mice survival probability increased in mice under immunotherapy with CCHA compared with CCHB, CCH and PBS treated mice (69.5 *vs* 64, 60 and 46.5 days, respectively). No allergic reactions or any toxic effects or visible metastases or organ lesions were observed in mice treated with either CCH subunits during the entire experiments.

## 4. Discussion

The relationship between the hemocyanin structure and the immunostimulatory activity that induce in mammals is still largely unknown. Previously, we demonstrated that hemocyanins that differ greatly in their origin and subunit organization, such as CCH and KLH, trigger similar immunostimulatory mechanisms: increased activity of natural killer cells, and a Th1 polarizing activity, without adding adjuvants. Therefore, we hypothesized that hemocyanins would induce an inflammatory reaction and stimulate the innate and adaptive immune response by common signals coded in their structure [30]. Knowing how hemocyanins are sending these signals to the mammal's immune system and the identification of their structural code in the molecule will be decisive for the better design of vaccines and to modulate the immune responses to treat cancer and autoimmunity. For that reason, we believe that is crucial to study the biochemical properties of each subunit of these giant proteins and to evaluate their potential adjuvanticity and therapeutical effect. With this purpose, first they should be free of cross contamination and characterized a fundamental requisite for molecules of pharmaceutical interest.

In the present study the immunogenicity of each subunits of *Concholepas* hemocyanin was investigated individually. Surprisingly, both subunits were found to be immunogenic, but with differences, without the need of adjuvant, similar to whole CCH. CCHA monomer immunized mice exhibited a higher antibody titer than CCHB monomer immunized mice. Furthermore since the hierarchy differs between mouse strains, it supports some type of genetic control of the immune response. In this regard, the genetic control of the response to KLH in mice seems to be under control of an autosomal dominant gene(s) that does not exert its effect at the level of antigen presenting cells, and it is not associated to MHC [46]. Therefore, the differences in the immunogenicity between CCHA and CCHB observed in different mice strains may be due to the intrinsic structural and biochemical differences between subunits.

In support of this line of thinking, the present study provides clear evidence that CCH subunits have profound structural differences. In the absence of full-length crystallographic data of the CCH subunits, the SERS methodology provides a very useful qualitative approach to obtain valuable structural information [47]. Most bands observed in the CCHA and CCHB spectra show different relative intensities and in some cases display slight frequency shifts (Table 1). The fact that the relative aminoacid abundance is similar in CCHA and CCHB [6] indicates that the observed intensity changes are mainly associated to conformational divergence from a common precursor that originated the heterodimeric subunit structure of the CCH. The presence of the amide III vibrations is consistent with peptide bonds of different energy along with the amide I vibration at 1625 $cm^{-1}$ and the skeletal mode at 925 $cm^{-1}$ is consistent with an α-helix conformation for the CCHA subunit [48]. The presence of a band at 1210 $cm^{-1}$ in all species could suggest the coexistence of an antiparallel β-sheet conformation [49]. Also, from the band widths in the CCH spectrum it can be inferred that its structure results from a single interaction between the CCHA and CCHB subunits rather than from a single or multiple interaction of each precursor. Thus, each subunit displays a particular conformation, being both independent as isolated systems; the vibrational spectrum of CCH as a whole, is a new spectrum, representing a new interaction of the subunits.

Additional significant information regarding the differences in hydrophilic properties of the CCH subunits arises from the SERS. If we assume that the aminoacids exposed on the molecule surface are those that likely interacting with the silver colloid, consequently, the subunit displays the more intense bands assigned to the more polar aminoacid correspond to the most hydrophilic polypeptide [50]. Accordingly, of special relevance is the spectra shown in Fig. 3 because it reveals that the CCHA might be more hydrophilic than the CCHB subunit. This deduction is in agreement with recently studies on the fluorescence emitted by exposed tryptophan residues on isolated subunits of *Concholepas* hemocyanin [51]. In addition, the presence of higher sugars content of CCHA (Table 2) makes it more hydrophilic. This property could be related to the higher immunogenicity of CCHA, facilitating its interaction with antigen presenting cells such as B lymphocytes, since the BCR primarily recognize epitopes in regions of relatively high segmental flexibility and hydrophilicity on the surface of proteins [52]. As a result, B-cells would be able to internalize and process CCHA more efficiently than CCHB in the endosomal class II-containing compartment, to prime naive T cells [53]. We speculate that the polyvalent and repetitive array of epitopes on FUs of CCH subunits could facilitate the capture by antigen-specific B cells of primed mice for the activation of CD4+ T cells. In fact, pre-immunization with hemocyanins before tumor inoculation is essential to the success of the immunotherapy in humans [17,18] and mice [30]. Indeed, in patients with urinary bladder cancer under intravesical KLH therapy, a delayed-type hypersensitivity reactions (DTH) occurs [54]. This type of responses is mediated by Th1 lymphocytes secreting IFNγ, a response associated with the generation of cellular immunity [30]. On the other hand, this suggests that its therapeutic properties could be attributable to a bystander effect on the antitumor response. This would occur through indirect stimulation of latent specific responses, either by breaking tolerance or by suppressing the immune reaction against the tumor. This is supported by the local secretion of cytokines like IFNγ, confirming a crucial role of hemocyanins in polarizing the cytokine environment to Th1 responses in the control of bladder cancer.

Others authors have suggested that the net charge of a protein must be a determinant factor in its interaction with cell surface receptor of DCs in own protein-models. In fact, it has been reported that a highly cationic protein, like chicken lysozyme (HEL) for instance, can be attached on the surface of DCs through electrostatic interactions with anionic surface molecules, thus stimulating HEL antigen specific receptor on B cells by DCs, and promoting HEL-specific B lymphocyte activation [55]. However, our data on p*I* and native electrophoresis of CCHA (Fig. 1D) are inconsistent with this view, because indicate that CCHA presents a greater net negative charge than CCHB. We hypothesize that this net charge condition is not decisive, because the interaction of CCHA subunits with cell surface receptors on DCs is a contribution and fine tuning of a combination of various factors, i.e., flexibility/mobility, accessibility, polarity, exposed surface, turns and antigenicity. This latter property is

relevant, because involucrate significantly the sugar components of mollusk hemocyanins: 3.2% of the molecular mass to KLH [56], and 3.1% to CCH, as shown the data obtained in the present work.

Today, the information regarding the carbohydrate moiety composition is essential for understanding the mollusk hemocyanin organization, antigenicity and their biomedical properties [57,58]. Concerning that DCs play a pivotal role in the generation of antitumor immune response, recently it has been proposed that KLH induce the maturation of DCs through their interaction with lectin-receptors, like mannose receptor [59]. Thus, we think if there are an ancient conserved immunogenic mechanism that is induced by KLH and CCH, it able to enhance Th1 immunity and leads to antitumor activity, the common signal might be in part, in some carbohydrate moieties on a subunit. To this respect, we demonstrated here, that CCH subunits differ in the nature and content of carbohydrates. Our results indicate that O-linked moiety is almost confined on the CCHA subunit. Similarly, in KLH has been demonstrated that the O-glycoside is restricted only to the KLH2-c subunit [60]. Interestingly, it has been suggested that O-linked glycoside, and specifically the presence in KLH2 subunit of the β-anomer of Gal (β1-3)-GalNac determinant as cross-reacting epitopes, is involved in the efficacy of KLH as an immunotherapeutic agent for the treatment of bladder carcinoma [61]. Accordingly, the antitumor activity of CCH subunits in a mice bladder cancer model showed that the incidence and the survival was better by using CCHA which is richer in O-linked glycoside moieties than CCHB. Unfortunately for comparative purposes, the immunostimulatory properties of the isolated KLH1 and KLH2 subunits by itself are not yet available. It has been reported that dissociated KLH subunits are less effective than multimeric KLH in immunotherapy experiments, but these studies were not fully conclusive [62]. On the other hand, recently it has been demonstrated that immunization with hemocyanin from *Rapana thomasiana* or its isolated subunits (RtH1 and RtH2), which are organized as homodecamers, similar to subunits of KLH, are immunogenic in mouse [63]. These results are in agree with our data reported here, demonstrating that neither the huge size, nor the $D_5$ symmetry of gastropod hemocyanins are involved in their immunologic properties, features that have been largely invoked to explain the immunogenicity of this colossal proteins.

Finally, in addition to known the individual contribution of CCHA and CCHB to *in vivo* immunogenic and antitumor effect related to their biochemical properties, our results raise the potential immunotherapeutic application of CCHA subunit since it is soluble and more homogeneous, while whole KLH and CCH are heterogeneous.

## Acknowledgements

This work was partially funded by Grants FONTEC-CORFO 2003-3816 (to Biosonda Corporation.) and FONDECYT 105-0150 (to M.I.B), and 107-0078 (to M.CV). We are thankful of the valuable help of the first grade students David Leiva, Felipe Schaerer, Daniela Díaz, Andrea Vera and Pablo Astudillo. Also, to the PhD students Sergio Arancibia and Francisco Vargas for their contributions to the discussion. We thank Dra. Casilda Mura from Millenium Institute ICYB, Universidad de Chile (UCH), by the critical revision of the manuscript. We thank Professors Jaime Eyzaguirre (UNAB) and Octavio Monasterio (UCH) for kindly providing some reagents and equipments. We thank Alejandro Munizaga from Servicio de Microscopía Electrónica (PUC) for their outstanding technical assistance. Also, we acknowledge Gabriel De Ioannes for his valuable helpful in figure preparation.

## References

[1] van Holde KE, Miller KI. Hemocyanins. Adv Protein Chem 1995;25:1–8.
[2] van Holde KE, Miller KI, Decker H. Hemocyanins and invertebrate evolution. J Biol Chem 2001;276:15563–6.
[3] Mellema JE, Klug A. Quaternary structure of gastropod haemocyanin. Nature 1972;239:146–51.
[4] Orlova EV, Dube P, Harris JR, Beckman E, Zemlin F, Markl J, et al. Structure of keyhole limpet hemocyanin type 1 (KLH1) at 15 Å resolution by electron cryomicroscopy and angular reconstitution. J Mol Biol 1997;271:417–37.
[5] Gebauer W, Harris JR, Heid H, Üling SM, Hillenbrand R, Söhngen S, et al. Quaternary structure, subunits and domain patterns of two discrete forms of keyhole limpet hemocyanin: KLH1 and KLH2. Zoology 1994;98:51–8.
[6] De Ioannes P, Moltedo B, Oliva H, Pacheco R, Faunes F, De Ioannes AE, et al. Hemocyanin of the molluskan *Concholepas concholepas* exhibits an unusual heterodecameric array of subunits. J Biol Chem 2004;279:26134–42.
[7] Weigle WO. Immunochemical properties of hemocyanin. Immunochemistry 1964;1: 295–26102.
[8] Harris JR, Markl K. Keyhole limpet hemocyanin (KLH): a biomedical review. Micron 1999;30:597-23.
[9] Musselli C, Livingstone PO, Rapugathi GJ. Keyhole limpet hemocyanin conjugate vaccine against cancer: the memorial Sloan Kettering experience. J Cancer Res Clin Oncol 2001;127(Suppl 2):R20–6.
[10] Kagan R, Rapupathi G, Yi SS, Reis CA, Gildersleeve J, Kahne D, et al. Comparison of antigen constructs and carrier molecules for augmenting the immunogenicity of the monosaccharide epithelial cancer antigen Tn. Cancer Immunol Immunother 2005;54:424–30.
[11] Sorensen AL, Reis CA, Tarp MA, Mandel U, Ramachandran K, Sankaranarayanan V, et al. Chemoenzymatically synthesized multimeric Tn/STn MUC1 glycopeptides elicit cancer-specific anti-MUC1 antibody responses and override tolerance. Glycobiology 2006;16:96-07.
[12] Gatza E, Okada CY. Tumor cell lysate-pulsed dendritic cells are more effective than TCR Id protein vaccines for active immunotherapy of T Cell Lymphoma. J Immunol 2002;169:5227–35.
[13] Timmerman JM, Levy R. Linkage of foreign carrier protein to a self-tumor antigen enhances the immunogenicity of a pulsed dendritic cell. J Immuno1 2000;64: 4797-03.
[14] Benchereau J, Ueno H, Dhodapkar M, Connolly J, Finholt JP, Klechevsky E, et al. Immune and clinical outcomes in patients with stage IV melanoma vaccinated with peptide-pulsed dendritic cells derived from CD34+ progenitors and activated with type I interferon. J Immunother 2005;28:505–16.
[15] Escobar A, López M, Serrano A, Ramírez M, Pérez C, Aguirre A, et al. Dendritic cell immunization alone or combined with low doses of interleukin-2 induce specific immune responses in melanoma patients. Clin Exp Immunol 2005;142:555–68.
[16] Redman BG, Chang AE, Whitfield J, Esper P, Jiang G, Braun T, et al. Phase Ib trial assessing autologous, tumor-pulsed dendritic cells as a vaccine administered with or without IL-2 in patients with metastatic melanoma. J Immunother 2008;31: 591–8.
[17] Jurincic-Winkler CD, Metz KA, Beuth J, Klippel KF. Keyhole limpet hemocyanin for carcinoma in situ of the bladder: a long-term follow-up study. Eur Urol 2000;37: 45–9.
[18] Lamm DL, Dehaven JI, Riggs DR. Keyhole limpet hemocyanin immunotherapy of bladder cancer: laboratory and clinical studies. Eur Urol 2000;37(Suppl 3):41–4.
[19] Gathuru JK, Koide F, Rapupathi GJ, Adams L, Kerns RT, Coleman TP, et al. Identification of DHBcAg as a potent carrier protein comparable to KLH for augmenting MUC1 antigenicity. Vaccine 2005;23:4727–33.
[20] Oliva H, Moltedo B, De Ioannes P, Faunes F, De Ioannes AE, Becker MI. Monoclonal antibodies to molluskan hemocyanin from *Concholepas concholepas* demonstrate common and specific epitopes among subunits. Hybrid Hybridomics 2002;21: 365–74.
[21] Swerdlow RD, Ratliff TL, La Regina M, Ritchey JK, Ebert RF. Immunotherapy with keyhole limpet hemocyanin: Efficacy and safety in the MB-49 intravesical murine bladder tumor model. J Urol 1994;151:1718–22.
[22] Leyton P, Lizama-Vergara PA, Campos-Vallette MM, Becker MI, Clavijo E, Córdova-Reyes IC et al. Surface enhanced Raman spectrum of nanometric molecular systems. J Chil Chem Soc 1005;50:725-30.
[23] Duvillie B, Attali M, Aiello V, Quemeneur E, Scharfmann R. Label-retaining cells in the rat pancreas. Location and differentiation potential *in vitro*. Diabetes 2003;52: 2035–42.
[24] Manosalva H, De Ioannes AE, Becker MI. Development of monoclonal antibodies bearing the internal image of the gizzerosine epitope an application in a competitive ELISA for fish meal. Hybrid Hybridomics 2004;23:45-4.
[25] Cancino J, Torrealba C, Soza A, Yuseff MI, Gravotta D, Henklein P, et al. Antibody to AP1B adaptor blocks biosynthetic and recycling routes of basolateral proteins at recycling endosomes. Mol Biol Cell 2007;18:4872–84.
[26] Matus S, Burgos PV, Bravo-Zehnder M, Kraft R, Porras OH, Kraft OH, Farías P, et al. Antiribosomal-P autoantibodies from psychiatric lupus target a novel neuronal surface protein causing calcium influx and apoptosis. J Exp Med 2007;204:3221–34.
[27] Miller LA, Talwar GP, Killian GJ. Contraceptive effect of a recombinant GnRH vaccine in adult female pigs. In: Timm RM, O'Brien JM, editors. Proc. 22nd Vertebr. Pest. Conf. Davis: Published at Univ. of Calif; 2006. p. 106–9.
[28] Pilon J, Loiacono C, Okeson D, Lund S, Vercauteren K, Rhyan J, et al. Anti-prion activity generated by a novel vaccine formulation. Neurosci Lett 2007;429:161–4.
[29] Becker MI, De Ioannes AE, León C, Ebensperguer L. Females of the communally breeding rodent, *Octodon degus*, transfer antibodies to their offspring during pregnancy and lactation. J Reprod Immunol 2007;74:68-7.
[30] Moltedo B, Faunes F, Haussmann D, De Ioannes P, De Ioannes AE, Puente J, et al. Immunotherapeutic effect of *Concholepas* hemocyanin in the murine bladder cancer model: evidence for conserved antitumor properties among hemocyanins. J Urol 2006;176:2690–5.

[31] Bradford MM. A rapid and sensitive for the quantitation of microgram quantities of protein utilizing the principle of protein-dye binding. Anal Biochem 1976;72: 248–54.
[32] De Ioannes P, Peirano A, Steiner J, Eyzaguirre J. An alpha-L-arabinofuranosidase from *Penicillium purpurogenum*: production, purification and properties. J Biotechnology 2000;76:253–8.
[33] Laemmli UK. Cleavage of structural proteins during the assembly of the head of bacteriophage T4. Nature 1970;227:680–5.
[34] Morrisey JH. Silver stain for proteins in polyacrylamide gels: a modified procedure with enhanced uniform sensitivity. Anal Biochem 1981;117:307–10.
[35] Valenzuela MA, Gamarra N, Gómez L, Kettlun AM, Sardon M, Pérez LM, et al. A comparative study of fish species identification by isoelectrofocusing, two-dimensional gel electrophoresis, and capillary zone electrophoresis. J Cap Electrophor Microchip Technol 1999;6:85–91.
[36] Walker JM. Two-dimensional immunoelectrophoresis. In: Walker JM, editor. The Protein Protocols Handbook. Totowa, New Jersey, USA: Humana Press Inc; 1996. p. 763–8.
[37] Keller H, Lieb B, Altenhein B, Gebauer D, Richter S, Stricker S, et al. Abalone (*Haliotis tuberculata*) hemocyanin type (HtH1). Organization of the approximately 400 kDa subunit, and amino acid sequence of its functional units f, g and h. Eur J Biochem 1999;264:27–8.
[38] Towbin HE, Staehelin T, Gordon J. Electrophoretic transfer of proteins from polyacrylamide gels to nitrocellulose sheets: procedure and some applications. Proc Natl Acad Sci U S A 1979;76:4350–4.
[39] Hounsell EF, Davies MJ, Smith KD. Chemical methods of analysis of glycoproteins. In: Walker JM, editor. The Protein Protocols Handbook. Totowa, New Jersey, USA: Humana Press Inc; 1996. p. 633–7.
[40] Hermanson GT. Bioconjugate techniques. USA: Academic Press Inc; 1996.
[41] Spiro R, Bhoyroo V. Structure of the O-glycosidically linked carbohydrate units of fetuin. J Biol Chem 1974;249:5704–17.
[42] Savage D, Mattson G, Desai S, Nielander G, Morgensen S, Conklin E. Avidin–biotin chemistry: a handbook. Rockford IL, USA: Pierce Chemical Company; 1992.
[43] Crowther J, Abu-Elzeein E. Detection of antibodies against foot-and-mouth disease virus using purified *Staphylococcus* A protein conjugated with alkaline phosphatase. J Immunol Methods 1980;34:261–7.
[44] Wormald MR, Dwek R. Glycoproteins: glycan presentation and protein-fold stability. Structure 1999;7:R155–60.
[45] Linn JF, Black P, Derksen K, Rübben H, Thüroff JW. Keyhole limpet haemocyanin in experimental bladder cancer. Literature review and own results. Eur Urol 200;37 (suppl 3):34–40.
[46] Cerottini JC, Unanue ER. Genetic control of the immune response of mice to hemocyanin. I. The role of macrophages. J Immunol 1971;106:732–9.
[47] Pavan Kumar GV, Ashok A, Reddy M, Arif T, Kundu K, Narayana C. Surface-enhanced Raman scattering studies of human transcriptional coactivator p300. J Phys Chem 2006;110:16787–92.
[48] Cuff ME, Miller KI, van Holde KE, Hendrickson WA. Crystal structure of a functional unit from *Octopus* hemocyanin. J Mol Biol 1998;278:855–70.
[49] Mouche F, Zhu Y, Pulokas J, Potter CS, Carragher B. Automated three-dimensional reconstruction of keyhole limpet hemocyanin type 1. J Struc Biol 2003;144: 301–12.
[50] Campos-Vallette M. In: Zagal JH, Bedioui F, Dodelet JP, editors. $N_4$-macrocyclic metal complexes. New York: Springer; 2003. p. 725–90.
[51] Idakieva K, Nikolov P, Chakarska I, Genov N, Shnyrov VL. Spectroscopic properties and conformational stability of *Concholepas concholepas* hemocyanin. J Fluoresc 2008;18:715–25.
[52] Hopp TP, Woods KR. Prediction of protein antigenic determinants from amino acid sequences. Proc Natl Acad Sci U S A 1981;78:3824–8.
[53] Lanzavecchia A. Receptor-mediated antigen uptake and its effect on antigen presentation to class II-restricted T lymphocytes. Annu Rev Immunol 1990;8:773–93.
[54] Jurincic-Winkler CK, Metz A, Beuth J, Engelman U, Klippel KF. Immunohistological findings in patients with superficial bladder carcinoma after intravesical instillation of keyhole limpet haemocyanin. Br J Urol 1995;76 702–.
[55] Qi H, Egen JG, Huang AYC, Germain RN. Extrafollicular activation of lymph node B cells by antigen-bearing dendritic cells. Science 2006;312:1672–6.
[56] Siddiqui NI, Idakieva K, Demarsin B, Doumanova L, Compernolle F, Gielens C. Involvement of glycan chains in the antigenicity of *Rapana thomasiana* hemocyanin. Biochem Biophys Res Comm 2007;361:705–11.
[57] Kurokawa T, Wuhrer M, Lochnit G, Geyer H, Markl J, Geyer R. Hemocyanin from the keyhole limpet *Megathura crenulata* (KLH) carries a novel type of N-glycans with Gal(β1-6)man-motifs. Eur J Biochem 2002;269:5459–73.
[58] Paccagnella M, Bologna L, Beccaro M, Micetic I, Di Muro P, Salvato B. Structural subunit organization of molluscan hemocyanins. Micron 2004;35:21–2.
[59] Presicce P, Taddeo A, Conti A, Villa ML, Bella SD. Keyhole limpet hemocyanin induces the activation and maturation of human dendritic cells through the involvement of mannose receptor. Mol Immunol 2008;45:1136–45.
[60] Stoeva S, Schütz J, Gebauer W, Hundsdörfer T, Manz C, Markl J, et al. Primary structure and unusual carbohydrate moiety of functional unit 2-c of keyhole limpet hemocyanin (KLH). Biochim Biophys Acta 1999;1435:94-09.
[61] Wirguin I, Suturkova-Milosevic L, Briani C, Latov N. Keyhole-limpet hemocyanin contains Gal(beta 1-3)-GalNac determinants that are cross-reactive with the T antigen. Cancer Immunol Immunother 1995;40:307–10.
[62] Swerdlow RD, Ebert RF, Bonaventura C, Miller KI. KLH: structural and functional characterization of two different subunits and multimers. Comp Biochem Physiol B Biochem Mol Biol 1996;113:537–48.
[63] Tchorbanov A, Idakieva K, Mihaylova N, Doumanova L. Modulation of the immune response using *Rapana thomasiana* hemocyanin. Intern Immunopharmacol 2008;8: 1033–8.